Shape-Selective Synthesis and Facet-Dependent Enhanced Electrocatalytic Activity and Durability of Monodisperse Sub-10 nm Pt−Pd Tetrahedrons and Cubes

An-Xiang Yin,[†] Xiao-Quan Min,[†] Ya-Wen Zhang,* and Chun-Hua Yan*

Beijing National Laboratory for Molecular Sciences, State Key Laboratory of Rare Earth Materials Chemistry and Applications, PKU-HKU Joint Laboratory in Rare Earth Materials and Bioinorganic Chemistry, College of Chemistry and Molecular Engineering, Peking University, Beijing 100871, China

S *Supporting Information*

ABSTRACT: Monodisperse single-crystalline sub-10 nm Pt−Pd nanotetrahedrons (NTs) and nanocubes (NCs) were synthesized with high shape selectivity via one-pot hydrothermal routes with small ions as efficient facet-selective agents. These alloy nanocrystals showed facet-dependent enhanced electrocatalytic activity and durability for methanol electrooxidations with commercial Pt/C catalyst as a reference. The (100)-facet-enclosed Pt−Pd NCs demonstrated a higher activity, whereas the (111)-facet-enclosed Pt−Pd NTs exhibited a better durability.

Shape-controlled synthesis of metal nanocrystals lends several unique properties to these key materials applied in catalysis,[1] sensing,[2] imaging,[3] electronics,[4] and photonics,[5] etc. Among these metals, Pt-based nanocrystals are a kind of the fundamental catalysts widely used in fuel cells,[6] petroleum cracking,[1] and hydrogenation,[7] etc. The shape control of Pt-based nanocrystals has drawn growing interest due to the achievements in tuning the catalytic activity and selectivity by modifying the exposing facets (including the three basal (100), (110), and (111) facets[7,8] and several high index facets[9]) of the nanocrystals in a series of catalytic reactions. Recently, it is further recognized that the preparation of Pt-based bimetallic Pt−M (M = Pd, Fe, Co, Ni, Cu, Mn, etc.) nanocrystals[10] was an efficient way to obtain active and durable catalysts with less consumption of expensive Pt metals. However, it is still a significant challenge to realize the fine shape control of Pt-based nanocrystals with multimetal compositions.[11] Generally, the shape control of metal nanocrystals in solutions can be achieved via the regulation of the relative growth rates of different facets[12] by means of (a) selective adsorption of different chemical species on specific crystal planes,[13] (b) delicate tuning of the nanocrystal growth regime (kinetically or thermodynamically),[14] and (c) epitaxial growth from seeds with predefined morphologies.[15]

So far, only limited reports have been devoted to the shape-control of Pt−Pd nanocrystals. For instance, Pt−Pd hollow nanostructures,[16] core−shell structures,[15,17] alloyed nanocubes,[18] and heterostructures[19] with superior catalytic activities toward both electroctalytic and heterogeneous catalytic reactions have been prepared by various solution methods such as hydrothermal treatment,[16,18] polyol reaction,[17] and seeded growth.[15,19] Herein, we report a shape-selective synthesis of monodisperse single-crystalline sub-10 nm Pt−Pd nanotetrahedrons (NTs) and nanocubes (NCs)

with facet-dependent enhanced electrocatalytic activity and durability toward methanol electrooxidations. In this hydrothermal protocol (Scheme 1), some small ions and poly(vinylpyrrolidone) (PVP) were employed as facet-selective ((100) or (111)) agents and capping ligands, respectively.

With the combined use of $Na_2C_2O_4$ and formaldehyde as the (111)-facet selective agent and reductant, single-crystalline Pt−Pd NTs enclosed by four (111) facets with a shape selectivity of ∼70% and a size distribution of 4.9 ± 0.5 nm could be obtained (Figures 1a,c and S1 in Supporting Information (SI)). While uniform single-crystalline Pt−Pd NCs (8.5 ± 0.8 nm) with a shape selectivity of ∼88% could be prepared with the mixture of large amount of Br^- and tiny amount of I^- anions as the (100) facet-selective agents (Figures 1b,d and S2 in SI). XRD patterns of both the Pt−Pd NTs and NCs agreed well with the standard data of fcc Pt and Pd (Figure S3 in SI). The broadened peaks for NTs demonstrated the ultrasmall sizes of the particles; while the enhanced relative intensity of the (200) peak to the (111) peak for Pt−Pd NCs (as compared to Pt−Pd NTs) further confirmed that the Pt−Pd NCs were surrounded by the (100) planes.[8c] The molar ratios of Pt/Pd in Pt−Pd NTs and NCs were determined by both inductively coupled plasma−atomic emission spectrometry (ICP-AES) analysis (Pt/Pd = 45:55 and 46:54 for Pt−Pd NTs and NCs, respectively) and energy dispersive X-ray spectroscopy (EDS) (Pt/Pd = 46:54 and 47:53 for Pt−Pd NTs and NCs, respectively; Figures S1b and S2b in SI) agreeing with the calculated molar ratio (1:1) from the Pt and Pd precursors. Distributions of Pt/Pd elements in a single Pt−Pd NT or NC were measured with high-angle annular dark-field scanning transmission electron microscopy-energy dispersive X-ray spectroscopy (HAADF-STEM-EDS) line scan analysis. Although the surface energy of Pd (2.05 J/m^2) is lower than that of Pt species (2.48 J/m^2),[20] no obvious segregation of Pt or Pd species was observed in Pt−Pd NTs or NCs (Figure 1e,f, insets), suggesting the quasi-homogeneous distributions of Pt/Pd elements throughout the whole particles along with the formation of alloy structures for the nanocrystals, as also confirmed by the XPS measurements for Pt−Pd NCs (Pt/Pd = 44:56, Figure S4 in SI).

Considering the poor facet-selective capability of PVP on sub-10 nm Pt−Pd nanocrystals (Figure S5 in SI),[11b] the stabilization effect of $C_2O_4^{2-}$ species on the (111) facet was ascribed to be the key factor for the formation of regularly shaped Pt−Pd NTs

Scheme 1. Shape-Selective Synthesis of Pt−Pd NTs and NCs

Figure 2. (a) Stable CV curves obtained for the Pt−Pd NCs, NTs, and Pt/C in the electrolyte of 0.1 M $HClO_4$ and 1 M CH_3OH at the sweep rate of 50 mV/s. (b) CV curves obtained after 4000 additional cycles.

solution (40%) was increased from 0.2 to 0.4 mL (Figures S6e in SI and 1a), whereas the further increase of formaldehyde solution (40%) to 0.8 mL would not have significant effects on the shape selectivity and size distribution of the as-prepared Pt−Pd NTs (Figure S6f in SI). Thus, the combination of appropriate amounts of $C_2O_4^{2-}$ and formaldehyde species is responsible for the formation of regularly shaped Pt−Pd NTs with high shape selectivity and narrow size distribution in the synthesis.

In the synthesis of Pt−Pd NCs with the (100) facet stabilized by the cooperation effects of Br^- and I^- species,[11,16] PVP was employed as an alternative reductant since formaldehyde was found to have a negative effect on the formation of regularly shaped Pt−Pd NCs (Figure S7a in SI) due to the possible strong adsorption of several intermediate chemical species decomposed from formaldehyde on the (111) surfaces.[22] Interestingly, the mixed surface adsorption agents of large numbers of Br^- and small numbers of I^- anions were proved to be critical for the formation of Pt−Pd NCs. On the one hand, neither could Pt−Pd NCs be prepared without any Br^- or I^- species (Figure S7b in SI), nor could Pt−Pd NCs with sharp corners be obtained with abundant Br^- but no/insufficient I^- species (Figure S7c,d in SI), proving the stronger surface-stabilizing ability of I^- than that of Br^-.[16] On the other hand, no well-dispersed Pt−Pd NCs but large agglomerations of small cubic-shaped nanocrystals could be obtained instead, due to the possibly too strong affinity of large numbers of I^- to the (100) facet of Pt−Pd NCs (Figure S7e,f in SI), as further demonstrated by the XPS analysis (Figure S4 in SI) for the as-obtained Pt−Pd NCs (Determined: Pt/Pd/Br/I = 44:56:10:11; calculated: Pt/Pd/Br/I = 50:50:2500:5).

The catalytic performance of the Pt−Pd NTs and NCs toward methanol electrooxidation was carried out with a three-electrode system in the electrolytes of 0.1 M $HClO_4$, 1 M CH_3OH under N_2 protection at room temperature (Figure 2). All potentials of the cyclic voltammetry (CV) measurements were converted to the values reversible hydrogen electrode (RHE) values, and all current density values were normalized to the electrochemically active surface area estimated from the hydrogen adsorption−desorption charges. CV curves of commercial Pt/C catalyst (Pt nanoparticles: <3.5 nm, Figure S8 in SI) were also included for comparison. Both the Pt−Pd NCs and NTs showed high catalytic activities toward methanol electrooxidation in the order of Pt−Pd NCs > NTs > Pt/C. The peak voltage values (E_f) and the peak current density values (J_f) in a forward (positive) scan were respectively 0.85 V and 1.49 mA/cm^2 for Pt−Pd NCs and respectively 0.84 V and 1.12 mA/cm^2 for Pt−Pd NTs, as compared with the respective values of 0.85 V and 0.51 mA/cm^2 for Pt/C. Furthermore, the ratio of the current density values in two sequential forward and backward (negative) sweeps (J_f/J_b) (as considered to be an important indicator of the catalyst tolerance to poisoning species,[23]) showed significant differences
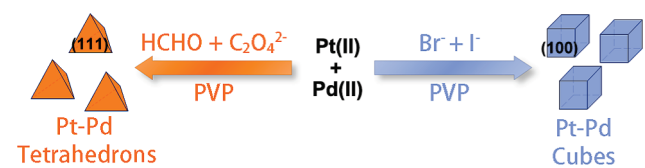

Figure 1. TEM images of the Pt−Pd NTs (a) and NCs (b), HRTEM images of a single Pt−Pd NT (c) and NC (d), and HAADF-STEM images of Pt−Pd NTs (e) and NCs (f). Insets in panels a and b are the size distribution histograms of the as-prepared NTs and NCs, respectively. Insets in panels e and f are the HAADF-STEM-EDS line scan profiles of a single NT and NC highlighted with a red line in panels e and f, respectively.

instead of those thermodynamically stable Wulff's polyhedrons at the sub-10 nm scale (Figure S6a−c in SI).[21] The use of a certain amount of formaldehyde as a reductant could provide a fast enough reducing rate to improve the shape- and size-uniformity of the as-prepared Pt−Pd NTs (Figure S6d−f in SI). In the absence of formaldehyde, no uniform Pt−Pd NTs but differently shaped single-crystalline and multi-twinned nanocrystals were obtained with the selectivity of ∼10% for NTs (Figure S6d in SI). Furthermore, the shape selectivity of Pt−Pd NTs would increase from ∼50% to ∼70%, and the particle size would decrease from 6.2 ± 0.5 nm to 4.9 ± 0.5 nm when the amount of formaldehyde
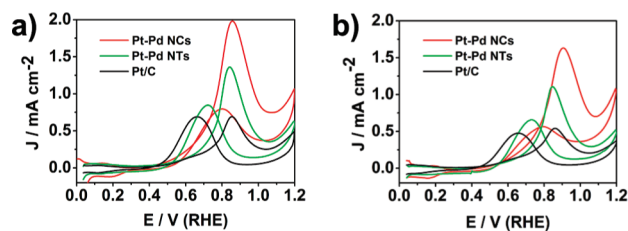
3817

dx.doi.org/10.1021/ja200329p |*J. Am. Chem. Soc.* 2011, 133, 3816–3819

for these three samples. The J_f/J_b values were 2.5, 1.4, and 0.8 for Pt−Pd NCs, NTs and Pt/C, respectively. Thus, both the Pt−Pd NCs and NTs exhibited much better tolerance to the poisoning species than the Pt/C catalyst despite the fact that the carbon support would enhance the performance of Pt/C catalysts toward methanol oxidation.[24] In addition, the durability of the as-prepared Pt−Pd NCs, NTs and Pt/C were tested by repeating the CV sweeps for over 4000 cycles (Figures 2b and S9 in SI). The activities of both Pt−Pd NCs and NTs remained higher than Pt/C even after an additional 4000 sweeping cycles. The J_f values for Pt−Pd NCs and NTs were 0.98 and 0.91 mA/cm^2, respectively, showing the loss of activities of 33% and 18%, respectively, as compared with the loss of 22% for Pt/C (0.40 mA/cm^2 after 4000 cycles). The E_f values for Pt−Pd NCs and Pt/C rose to 0.90 and 0.87 V after 4000 cycles while the E_f value for Pt−Pd NTs remained at 0.84 V, showing a better durability of the Pt−Pd NTs than Pt−Pd NCs and Pt/C.

The observed enhancement of both activity and tolerance to the poisoning species for the Pt−Pd NTs and NCs could be ascribed to the formation of bimetallic surface atom arrangements (coexistence of surface Pd and Pt sites)[18,25] and/or the modification of the electronic structure of surface Pt atoms through the alloying with Pd atoms.[26] The different J_f/J_b values for Pt−Pd NCs (2.5) and NTs (1.4) indicated that different reaction pathways might be adopted on the (100) or (111) surfaces,[27] and the reason for the better durability of Pt−Pd NTs could be ascribed to the more durable nature of the (111) facet of Pt-based nanocrystals, which was found in the electrooxidations of formic acid with Pt catalysts.[28] The different electrocatalytic performances of the Pt−Pd NCs and NTs demonstrated the facet-sensitive nature (i.e., structure-sensitivity) of methanol electrooxidation on Pt−Pd nanocrystals. The (100)-facet-enclosed NCs showed a higher catalytic activity than the (111)-facet-enclosed NTs, and the NTs preserved a better durability than the NCs, while both the NCs and NTs showed better catalytic performance than the Pt/C catalyst.

In conclusion, monodisperse single-crystalline sub-10 nm Pt−Pd NTs and NCs were prepared in high selectivity based on the concept of stabilizing particular facets with shape-selective small ions. The as-prepared nanocrystals preserved a superior electrocatalytic activity and durability for methanol electrooxidations to commercial Pt/C catalyst. The (100)-facet-enclosed Pt−Pd NCs showed a higher activity, while the (111)-facet-enclosed Pt−Pd NTs held a better durability. This work has not only provided new insights in shape-controlled synthesis of multimetal nanocrystals, but also opened up new opportunities for the testing of various structure-sensitive material properties of Pt−Pd nanocrystals with potential applications.

■ ASSOCIATED CONTENT

S **Supporting Information.** Experimental details, more TEM images, results of EDS, XRD, XPS analyses, and electrocatalysis data. This material is available free of charge via the Internet at http://pubs.acs.org.

■ AUTHOR INFORMATION

Corresponding Author
ywzhang@pku.edu.cn; yan@pku.edu.cn

Author Contributions
†These authors contributed equally.

■ REFERENCES

(1) (a) Somorjai, G. A. *Chem. Rev.* **1996**, *96*, 1223.(b) Ertl, G.; Knözinger, H.; Weitkamp, J. *Handbook of Heterogeneous Catalysis*; VCH: Weinheim, 1997. (c) Somorjai, G. A.; Li, Y. *Introduction to Surface Chemistry and Catalysis*, 2nd ed.; Wiley: Hoboken, NJ, 2010.

(2) Taton, T. A.; Mirkin, C. A.; Letsinger, R. L. *Science* **2000**, *289*, 1757.

(3) Yang, X. M.; Skrabalak, S. E.; Li, Z. Y.; Xia, Y. N.; Wang, L. H. V. *Nano Lett.* **2007**, *7*, 3798.

(4) Jeong, S.; Woo, K.; Kim, D.; Lim, S.; Kim, J. S.; Shin, H.; Xia, Y.; Moon, J. *Adv. Funct. Mater.* **2008**, *18*, 679.

(5) Maier, S. A.; Brongersma, M. L.; Kik, P. G.; Meltzer, S.; Requicha, A. A. G.; Atwater, H. A. *Adv. Mater.* **2001**, *13*, 1501.

(6) Steele, B. C. H.; Heinzel, A. *Nature* **2001**, *414*, 345.

(7) (a) Lee, H.; Habas, S. E.; Kweskin, S.; Butcher, D.; Somorjai, G. A.; Yang, P. D. *Angew. Chem., Int. Ed.* **2006**, *45*, 7824. (b) Bratlie, K. M.; Lee, H.; Komvopoulos, K.; Yang, P. D.; Somorjai, G. A. *Nano Lett.* **2007**, *7*, 3097.

(8) (a) Narayanan, R.; El-Sayed, M. A. *J. Am. Chem. Soc.* **2004**, *126*, 7194. (b) Narayanan, R.; El-Sayed, M. A. *Nano Lett.* **2004**, *4*, 1343. (c) Wang, C.; Daimon, H.; Onodera, T.; Koda, T.; Sun, S. H. *Angew. Chem., Int. Ed.* **2008**, *47*, 3588.

(9) Tian, N.; Zhou, Z. Y.; Sun, S. G.; Ding, Y.; Wang, Z. L. *Science* **2007**, *316*, 732.

(10) (a) Stamenkovic, V. R.; Mun, B. S.; Arenz, M.; Mayrhofer, K. J. J.; Lucas, C. A.; Wang, G. F.; Ross, P. N.; Markovic, N. M. *Nat. Mater.* **2007**, *6*, 241. (b) Xu, D.; Liu, Z. P.; Yang, H. Z.; Liu, Q. S.; Zhang, J.; Fang, J. Y.; Zou, S. Z.; Sun, K. *Angew. Chem., Int. Ed.* **2009**, *48*, 4217. (c) Zhang, J.; Fang, J. Y. *J. Am. Chem. Soc.* **2009**, *131*, 18543. (d) Wang, D. S.; Peng, Q.; Li, Y. D. *Nano Res.* **2010**, *3*, 574. (e) Kim, J.; Lee, Y.; Sun, S. H. *J. Am. Chem. Soc.* **2010**, *132*, 4996. (f) Kang, Y. J.; Murray, C. B. *J. Am. Chem. Soc.* **2010**, *132*, 7568.

(11) (a) Tao, A. R.; Habas, S.; Yang, P. D. *Small* **2008**, *4*, 310. (b) Xia, Y.; Xiong, Y. J.; Lim, B.; Skrabalak, S. E. *Angew. Chem., Int. Ed.* **2009**, *48*, 60.

(12) Wang, Z. L. *J. Phys. Chem. B* **2000**, *104*, 1153.

(13) Harris, P. J. F. *Nature* **1986**, *323*, 792.

(14) (a) Sun, Y. G.; Xia, Y. N. *Science* **2002**, *298*, 2176. (b) Tao, A.; Sinsermsuksakul, P.; Yang, P. D. *Angew. Chem., Int. Ed.* **2006**, *45*, 4597.

(15) Habas, S. E.; Lee, H.; Radmilovic, V.; Somorjai, G. A.; Yang, P. *Nat. Mater.* **2007**, *6*, 692.

(16) Huang, X. Q.; Zhang, H. H.; Guo, C. Y.; Zhou, Z. Y.; Zheng, N. F. *Angew. Chem., Int. Ed.* **2009**, *48*, 4808.

(17) Tao, F.; Grass, M. E.; Zhang, Y. W.; Butcher, D. R.; Renzas, J. R.; Liu, Z.; Chung, J. Y.; Mun, B. S.; Salmeron, M.; Somorjai, G. A. *Science* **2008**, *322*, 932.

(18) Yuan, Q.; Zhou, Z. Y.; Zhuang, J.; Wang, X. *Chem. Commun.* **2010**, *46*, 1491.

(19) (a) Lee, H. J.; Habas, S. E.; Somorjai, G. A.; Yang, P. D. *J. Am. Chem. Soc.* **2008**, *130*, 5406. (b) Lim, B.; Jiang, M. J.; Camargo, P. H. C.; Cho, E. C.; Tao, J.; Lu, X. M.; Zhu, Y. M.; Xia, Y. N. *Science* **2009**, *324*, 1302.

(20) Skriver, H. L.; Rosengaard, N. M. *Phys. Rev. B* **1992**, *46*, 7157.

(21) (a) Baletto, F.; Mottet, C.; Ferrando, R. *Phys. Rev. B* **2001**, 6315. (b) Baletto, F.; Ferrando, R.; Fortunelli, A.; Montalenti, F.; Mottet, C. *J. Chem. Phys.* **2002**, *116*, 3856. (c) Baletto, F.; Ferrando, R. *Rev. Mod. Phys.* **2005**, *77*, 371.

(22) (a) Huang, X. Q.; Tang, S. H.; Zhang, H. H.; Zhou, Z. Y.; Zheng, N. F. *J. Am. Chem. Soc.* **2009**, *131*, 13916. (b) Huang, X. Q.; Tang,

S. H.; Mu, X. L.; Dai, Y.; Chen, G. X.; Zhou, Z. Y.; Ruan, F. X.; Yang, Z. L.; Zheng, N. F. *Nat. Nanotechnol.* **2010**, *6*, 28.

(23) Mu, Y. Y.; Liang, H. P.; Hu, J. S.; Jiang, L.; Wan, L. J. *J. Phys. Chem. B* **2005**, *109*, 22212.

(24) Takasu, Y.; Kawaguchi, T.; Sugimoto, W.; Murakami, Y. *Electrochim. Acta* **2003**, *48*, 3861.

(25) (a) Watanabe, M.; Motoo, S. *J. Electroanal. Chem.* **1975**, *60*, 259. (b) Watanabe, M.; Motoo, S. *J. Electroanal. Chem.* **1975**, *60*, 267. (c) Watanabe, M.; Motoo, S. *J. Electroanal. Chem.* **1975**, *60*, 275.

(26) Nilekar, A. U.; Alayoglu, S.; Eichhorn, B.; Mavrikakis, M. *J. Am. Chem. Soc.* **2010**, *132*, 7418.

(27) (a) Jarvi, T. D.; Sriramulu, S.; Stuve, E. M. *Colloid Surf. A* **1998**, *134*, 145. (b) Housmans, T. H. M.; Wonders, A. H.; Koper, M. T. M. *J. Phys. Chem. B* **2006**, *110*, 10021. (c) Ferrin, P.; Mavrikakis, M. *J. Am. Chem. Soc.* **2009**, *131*, 14381.

(28) Markovic, N. M.; Ross, P. N. *Surf. Sci. Rep.* **2002**, *45*, 121.